J. Exp. Biol. (1970), **52**, 233–256
With 18 text-figures
Printed in Great Britain

LANDING REACTION OF *MUSCA DOMESTICA*:

DEPENDENCE ON DIMENSIONS AND POSITION OF THE STIMULUS

BY A. FERNANDEZ PEREZ DE TALENS
AND
C. TADDEI FERRETTI
Laboratorio di Cibernetica del C.N.R., Arco Felice (Napoli), Italy

(*Received* 12 *August* 1969)

INTRODUCTION

The functional structure of the mechanism underlying the perception of motion and its processing by the central nervous system has thus far been analysed in the beetle *Clorophanus viridis* (Hassenstein & Reichardt, 1956; Reichardt & Varjú, 1959; Reichardt, 1962), in the fly *Musca domestica* (Hertz, 1934*a*; Fermi & Reichardt, 1963; McCann & McGinitie, 1965; Bishop & Keehn, 1967) and in other compound-eye animals (Hertz, 1934*b*; Burtt & Catton, 1954; Horridge, 1966; Thorson, 1966; Wallace, 1959).

It is of interest therefore to ascertain whether such a mechanism is applied to the perception of more complicated dynamical features.

One environmental situation in which flying insects need the perception of one of such dynamical features is during their preparation for landing.

When a fly approaches a surface on which to land, at a certain distance from the surface it lifts its first pair of legs to both sides of the head and stretches the last pair backward. This characteristic behaviour has been called the landing reaction; it occurs not only in the house-fly but commonly in all flying insects.

Some investigations (Goodman, 1960, 1964; Braitenberg & Taddei Ferretti, 1966) of the landing reaction have proved that there are at least two components of the stimulus for landing. One of them is the expansion of a pattern on the fly's compound eye; and it is known that the greatest distance from the pattern at which the fly reacts is proportional to the expansion speed of the pattern. The other is the variation of the light flux coming from the pattern; and it is known that the fly reacts to the decrement of light flux.

Generally, patterns which can be expanded involve a change in light flux, thus preventing independent analysis of these two components of the stimulus. An example of such a stimulus is an object running up and away from the fly; change in object area, for a given contrast with the surrounding, involves a change in light flux. Another such stimulus is a cathode ray tube with expanding circles on its screen; the increase in the circumference of the circles increases the light flux.

In the present research the two components of the optical stimulus have been separated and the dependence of the landing reaction on each of them has been analysed.

METHODS

The present investigation concerns the dependence of the landing reaction on the speed of the expansion.

An expansion pattern which does not involve any change in the light flux is obtained (Taddei Ferretti & Fernandez Perez de Talens, 1967) by rotating—on its axis—a disk on which 2 m arithmetical spirals are drawn; these spirals are defined by $r(\theta) = p\theta/2\pi$, where r and θ are angular co-ordinates and p is the constant pitch. The pitches used vary between 1, 6 and 8 cm. Furthermore, the spirals are separated in phase by π/m (where m is an integer called multiplicity: the multiplicities used varying between 1 and 8) and the zones between one spiral and the next are alternately painted black and white. Such a disk will be specified by the values of p and m, and will be designated p/m.

When the fly is placed at a certain distance from a disk, in front of the centre of the disk, the reaction will take place only if the rotational frequency of the disk is higher than a minimum value ω.

If, alternatively, the rotational frequency is fixed, the fly reacts only if it stays at a certain distance from the disk which is smaller than a maximum value d.

Generally d and ω depend on the disk used:

$$d = d(\omega, p, m); \quad \omega = \omega(d, p, m).$$

In this paper the dependence of the landing reaction on geometrical characteristics of the stimuli has been analysed, and the efficiency of the stimulus as a function of its shape and of the stimulated zone in the visual field has been evaluated.

It is first necessary to ascertain that the pattern is of sufficient size. For this purpose

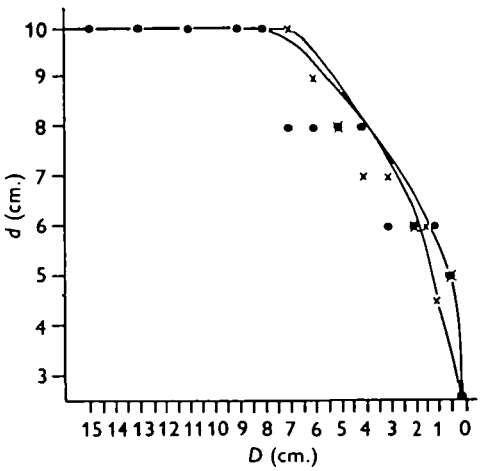

Fig. 1

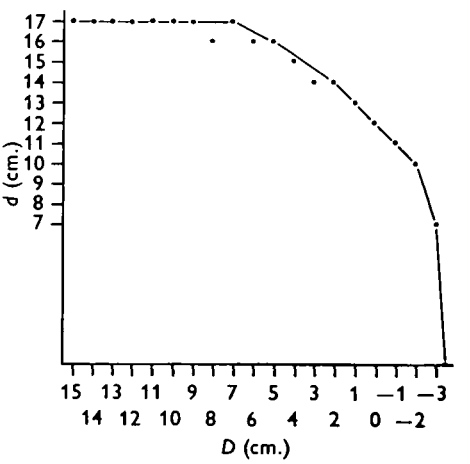

Fig. 2

Fig. 1. Dependence of threshold value d of fly-disk distance on the reduction of stimulating area. The reduction was obtained by covering two circular segments of the disk. The circular segments were limited by vertical chords at distance D from the centre; two flies; radial expansion speed V_R = 45 cm./sec.; spiral 8/5.

Fig. 2. Dependence of threshold value d of fly-disk distance on the reduction of stimulating area. The reduction was obtained by covering one circular segment of the disk. The circular segment was limited by a vertical chord at distance D from the centre; radial expansion speed V_R = 45 cm./sec.; spiral 8/5.

the exterior zones of the spiral are covered with cardboard masks having reflectivity intermediate between the reflectivities of the black and white zones of the spiral. Masks are used in succession as follows: two vertical masks on both sides of the disk (Fig. 1), one asymmetric mask (Fig. 2) and one annular mask having a fixed external diameter of 40 cm. and an internal diameter variable between 2 and 30 cm. (Fig. 3). All three procedures are used to determine a maximum efficiency radius whose value, although depending on the spiral pitch, is fully provided for in our disks; the criterion is that a further increase of the radius of the presented stimulus is not followed by a corresponding increase of the stimulus efficiency.

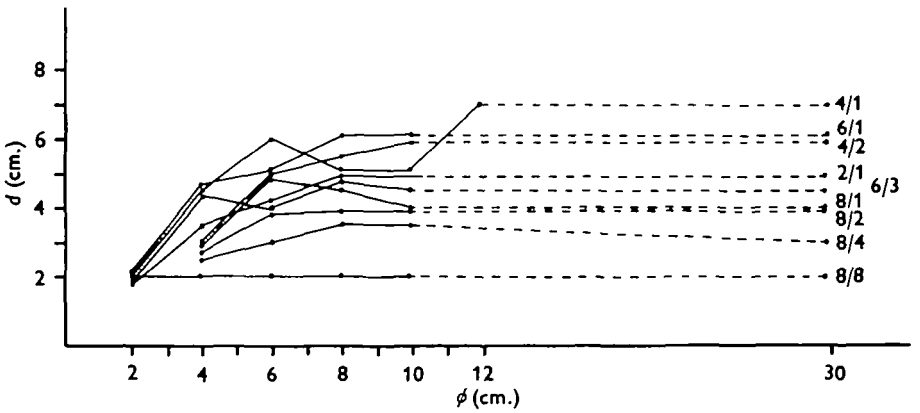

Fig. 3. Dependence of threshold value d of the fly-disk distance on the diameter ϕ of the stimulating disk.

RESULTS AND DISCUSSION

We first studied the dependence of the pattern efficiency on the spiral pitch and multiplicity. Each pattern has radial characteristics generating the expansion effect, but it has also tangential characteristics generating a tangential effect and a torsion effect which interfere with the expansion signal and decrease the stimulus efficiency. We have found that the stimulus efficiency depends on the frequency of the stimulus on each ommatidium. (First part.)

Secondly, we have analysed the Moiré effect. In our experiments on landing reaction no Moiré effect has been in any case noted; this fact (surprising because in the optomotor reaction of Diptera the Moiré effect occurs with a remarkable intensity (Götz, 1964)) is explained in terms of non-radial characteristics of the stimuli. (Second part.)

Finally, we have studied the dependence of the landing reaction on the stimulated area and on the position of the stimulus in the visual field of the fly, obtaining data on: (*a*) dependence on direction in which the pattern is presented; (*b*) isotropy of the fly's visual field; (*c*) discrimination between an expansion stimulus and a lateral displacement stimulus; (*d*) spatial integration of local landing stimuli, showing a spatial threshold for excitability and a spatial saturation effect. (Third part.)

First part

This first part refers to the dependence of d and ω on the pitch and on the multiplicity of the spiral.

If p is the pitch (cm.) of the spirals drawn on the rotating disk, and ω the rotational frequency of the disk (r.p.s.), the speed of the motion of the black and white zones along a radius (radial speed of expansion) will be $V_R = \omega p$ cm./sec.; in fact

$$r(\theta) = \frac{p\theta}{2\pi}; \quad \theta(t) = \theta_0 + 2\pi\omega t,$$

where t is time. Substituting

$$r(\theta, t) = \frac{p}{2\pi}(\theta_0 + 2\pi\omega t) = \frac{p\theta_0}{2\pi} + p\omega t;$$

then

$$V_R = \dot{r}(\theta, t) = \frac{\partial r}{\partial t}(\theta, t) = \omega p.$$

For each disk the diagrams showing the variation of d versus V_R and of V_R versus d are, for V_R up to 105 cm./sec., straight lines (see also Braitenberg & Taddei Ferretti, 1966). This shows a difference between landing reaction and optomotor reaction (Reichardt, 1962). In fact, as the angular speed of the stimulus is increased, the optomotor reaction increases, attains a maximum and then decreases, while the landing reaction continues to increase with the expansion speed. This could be explained in terms of different relations in the systems underlying the two types of reaction. If the optomotor stimulus speed is too high, it is unimportant for the fly to follow it; but the higher the speed of the stimulus to produce the landing reaction, the more important for the fly to be ready to land.

The fact that, with fixed p and m, d is a linear function of ω and the perceived expansion speed, for each disk, is constant ($V_p = \omega p/d = \text{const.}$) may lead one to think that V_p is always constant independently of the stimulating disk (i.e. that the whole dependence of ω and d on the geometrical characteristics of the disk is included in the linear dependence of V_R). In order to verify this hypothesis, many series of experiments have been performed by varying d, ω and p. It is to be noted that the same value of V_R may be obtained from spirals of different pitches by letting them rotate at angular speeds inversely proportional to the pitches $V_R = p_i\omega_i$, being $p_i : p_j = \omega_j : \omega_i$ for $i, j \in 1, \ldots, n$. It is also to be noted that all the disks with the same value of $L = p/m$ are radially equivalent, i.e. all of them show along a radius a sequence of alternate white and black zones of width $L/2$. Then it is not possible, by analysing only the modulation of the reflectivity along a radius, to discriminate between these disks or to distinguish them from disks with painted sets of alternate black and white circular rings of the same width $L/2$ and expanding at the same V_R. In fact, for any one of these disks and for a fixed value of V_R, we have, at each point and in the same time interval, the same number of changes black–white and the corresponding same perception of motion. In our experiments m also has been varied; for disks radially equivalent one may expect to find the same landing behaviour of flies.

But experimentally we find:

(i) For disks with the same $L = p/m$: (*a*) for a fixed V_R, by increasing the pitch and multiplicity, the maximum distance d, over which the fly never reacts, decreases;

(*b*) for a fixed *d*, by increasing the pitch and multiplicity, the minimum radial expansion speed V_R, under which the fly never reacts, increases (Fig. 4); then following from (*a*) and (*b*) above: (*c*) the minimum perceived expansion speed V_p, sufficient to generate a reaction, increases with the increase of the pitch and multiplicity, or, in other words, the stimulus loses its efficiency with the increase of the pitch and multiplicity.

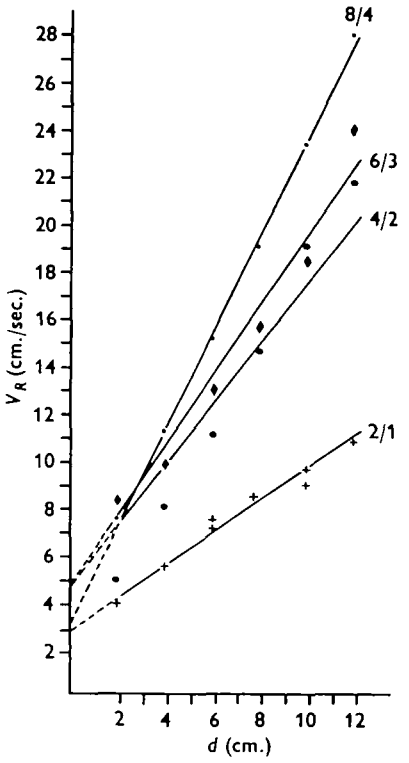

Fig. 4

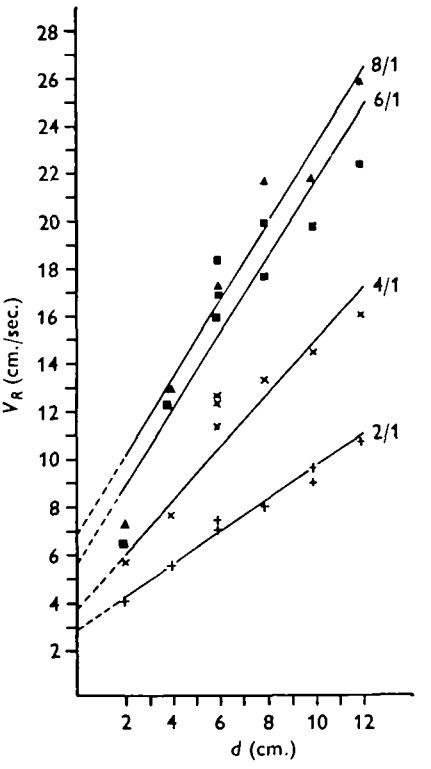

Fig. 5

Fig. 4. Dependence of threshold value V_R of radial expansion speed on the fly-disk distance *d*, for fixed $L = p/m = 2$ cm., and for variable pitches (p = 2, 4, 6, 8 cm.) and variable multiplicities (respectively m = 1, 2, 3, 4).

Fig. 5. Dependence of threshold value V_R of radial expansion speed on the fly-disk distance *d*, for fixed multiplicity (m = 1) and for variable pitches (p = 2, 4, 6, 8 cm.).

To establish whether this finding was due to the increase of p or to the increase of m, two more types of experiments have been performed:

(ii) Having fixed the multiplicity, for each value of the radial speed of expansion V_R we have investigated the dependence of the reaction on the pitch. Obviously this condition requires that the disks are not radially equivalent and that—in accordance with the results of investigations on the dependence of the optomotor reaction on the stimulus wavelength, showing an increase of stimulus efficiency with the increase of stimulus wavelength (Graffon, 1934; Fig. 6 of Fermi & Reichardt, 1963; Fig. 7 of Bishop & Keehn, 1967)—it could be expected that spirals with higher L (that is with higher p) would be more efficient. On the contrary, the results of this experiment show

that, in the same sense as above, the stimulus efficiency decreases with increasing pitch (Fig. 5).

(iii) Having fixed the pitch p, for each value of the radial speed of expansion V_R, we have investigated the dependence of the reaction on the multiplicity. For the same reason as in (ii), it could be now expected that spirals with higher L (that is, with lower m) would be more efficient. And in fact it has been found that, always in the same sense

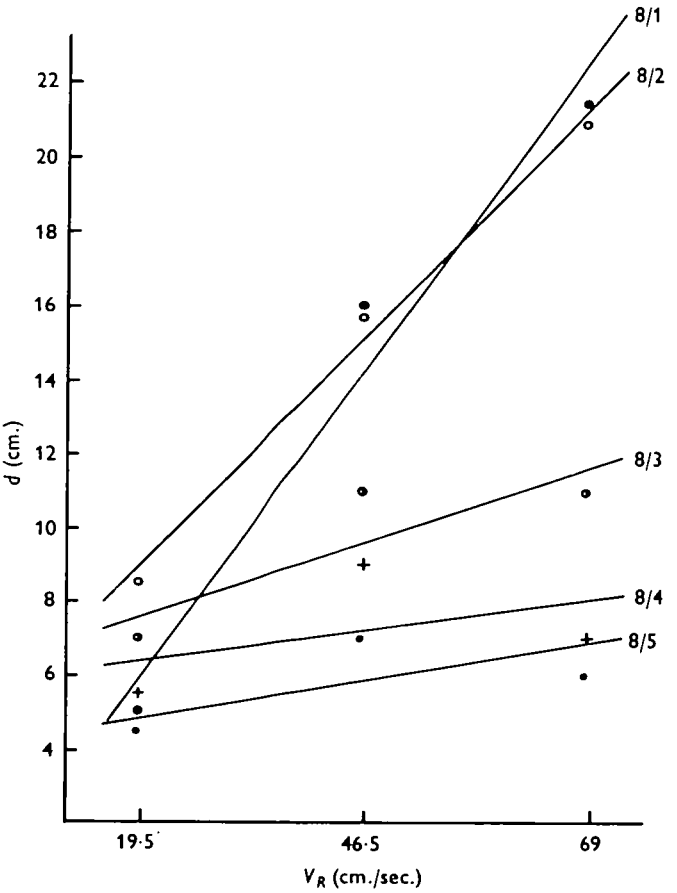

Fig. 6. Dependence of threshold value d of fly-disk distance on radial expansion speed V_R, for fixed pitch (p = 8 cm.) and for variable multiplicities (m = 1, 2, 3, 4, 5).

as above, the stimulus efficiency decreases with increasing multiplicity (Fig. 6). This would be in general obvious, because by increasing the multiplicity the pattern contrast decreases (Horridge, 1968) so diminishing the pattern efficiency; but in general our patterns are large enough.

All these results show that increases of p and m co-operate in generating the loss of efficiency in radially equivalent disks.

To explain the discrepancy between our results in (ii) and the results of authors mentioned above it is to be noted that a disk with a painted spiral causes, by rotating, the perception of an expansion in consequence of its radial characteristics, but that it causes also, in consequence of tangential characteristics, the perception of a tangential

displacement of the wave front, in the same sense as that of the disk rotation, as well as the perception, along each radius, of a torsion of the wave front in a sense opposite to that of the disk rotation. In fact, the direction of the wave front translation, normal to the wave front itself, is not a radial direction, but it is shifted of an angle $\mu = \tan^{-1} p/2\pi r$ (see Appendix 1); as can be seen, μ varies, increasing with the pitch and decreasing with the increase of the radius. The existence of such a μ produces the perception of a tangential displacement of the wave front (tangential effect). The variation of μ along the radius produces the perception of a torsion of the wave front (torsion effect). This variation is given by $\partial\mu/\partial r = -2\pi p/[(2\pi r)^2 - p^2]$ (see Appendix 1); as can be seen, the

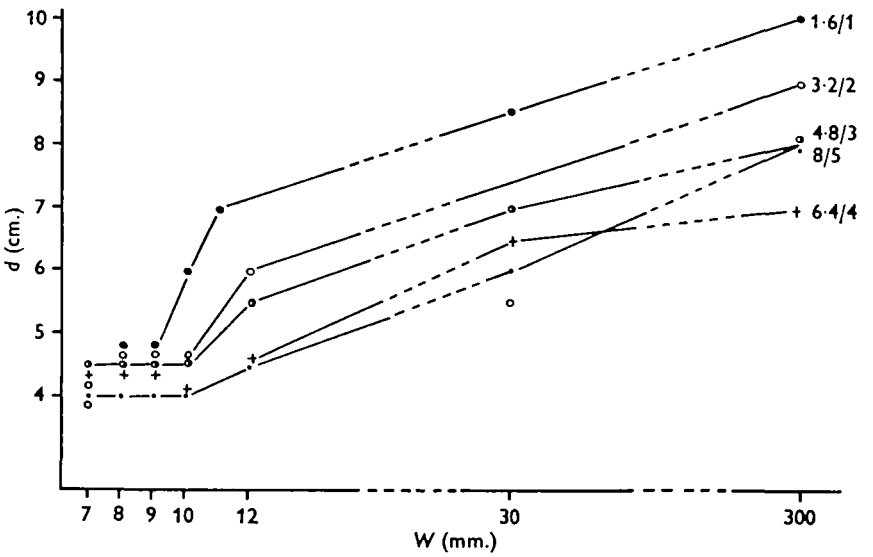

Fig. 7. Dependence of threshold value d of fly-disk distance on width w of a unidimensional stimulus (7–30 mm., and disk with a diameter of 30 cm.), for fixed $L = p/m = 1{\cdot}6$ cm., and for variable pitches ($p = 1{\cdot}6$, $3{\cdot}2$, $4{\cdot}8$, $6{\cdot}4$, $8{\cdot}0$ cm.) and variable multiplicities (respectively $m = 1, 2, 3, 4, 5$); radial expansion speed $V_R = 16$ cm./sec.

intensity of this torsion effect decreases with the increase of the radius and increases with the pitch. For a set of expanding circles, obviously $\mu = 0$ and $\partial\mu/\partial r = 0$, and the expansion would be purely radial. Thus the higher the pitch, the higher are μ and $\partial\mu/\partial r$ and the less comparable is the disk to the corresponding set of expanding circles. The tangential effect and the torsion effect have therefore to be considered as a form of interference on V_R, increasing with the pitch and decreasing with the increase of the radius. Further consideration of this interference and of other factors influencing the results of the above experiments is given in Appendix 2.

Considering what has been said hitherto, it appears logical that the whole dependence of d and ω on p is not included in the dependence on V_R, since the pitch influences not only the radial configuration of the spiral but also its tangential configuration.

A confirmation of this interpretation has been obtained through the following experiment. By sending the stimulus through a slit along a diameter, the perception of the angle μ and of $\partial\mu/\partial r$ may be eliminated. If the slit is widened, the intensity of perception of the parameters μ and $\partial\mu/\partial r$ increases, and, as a consequence, the scattering

between the curves corresponding to different pitches should increase. As can be seen in Fig. 7, the results of this experiment agree, qualitatively, with this interpretation.

Second part

A theoretical limit to the use of rotating spirals as expansion patterns could be the Moiré effect.

The Moiré effect consists in the fact that, when a moving periodic structure is observed by a periodic retina, the perceived motion does not ever coincide with the real one (Rayleigh, 1874).

Let ϕ be the interommatidic angle and 2λ the angle under which is seen the radial period of the stimulus; then if

$$(2\lambda)_n = 2\phi/n \quad (n = 1, \ldots)$$

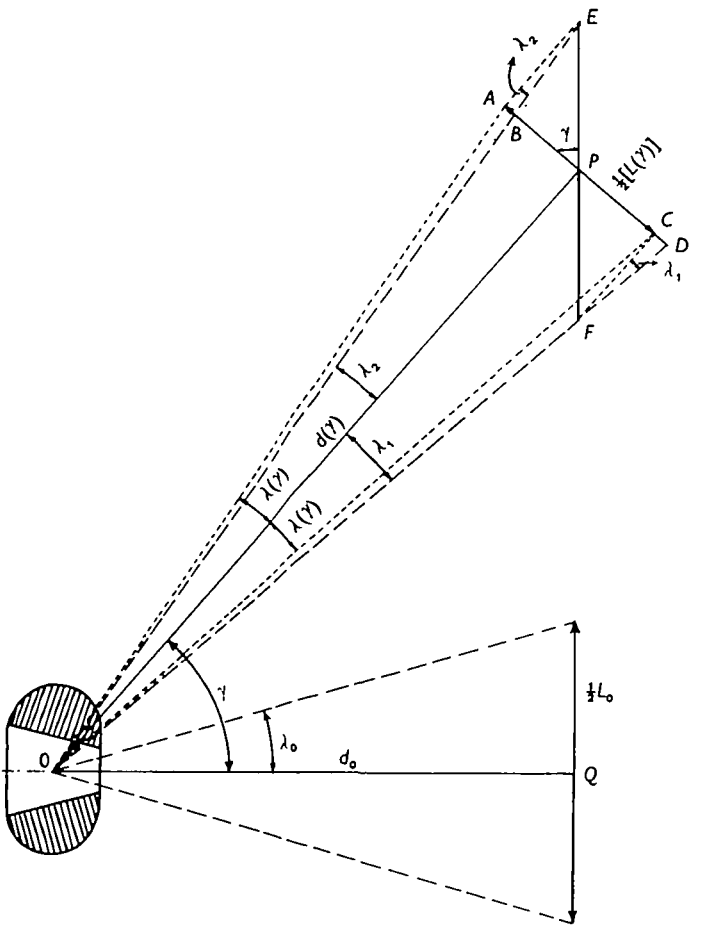

Fig. 8. Radial period of the spiral $[\lambda_1+\lambda_2]$ seen by an ommatidium whose axis is at angle γ with the fly-disk axis. $d_0 = d(0)$ = fly-disk distance. $d(\gamma)$ = fly-disk distance along the axis of an ommatidium whose axis is at angle γ with the fly-disk axis. $L_0 = L(0)$ = radial period of the spiral. $L(\gamma)$ = projection of the radial period of the spiral on the plane of an ommatidium whose axis is at angle γ with the fly-disk axis. λ_n = half of the radial period of the spiral seen along the fly-disk axis. $\lambda(\gamma)$ = projection of half of the radial period of the spiral on the plane of an ommatidium whose axis is at angle γ with the fly-disk axis as seen by that ommatidium.

the motion is not perceived at all; if 2λ lies between $(2\lambda)_{2n}$ and $(2\lambda)_{2n-1}$ ($n = 1, \ldots$) the sense of the motion, as perceived, is reversed; and finally the sense of the motion, as perceived, is the same—but not its speed—if 2λ lies between $(2\lambda)_{2n-1}$ and $(2\lambda)_{2n}$ ($n = 1, \ldots$).

The distance $d(\gamma)$ from an ommatidium—the axis of which forms an angle γ with the axis of the fly's head—to the observed point of the disk varies with γ according to $d(\gamma) = d_0/\cos\gamma$, where d_0 is the distance between the fly's head and the spiral (Fig. 8). On the other hand, the projection $L(\gamma)$ of the radial period of the spiral on the plane of the ommatidium varies with γ according to $L(\gamma) = L_0 \cos\gamma$, where L_0 is the radial period of the spiral.

So one half of the seen radial period of the spiral varies with γ according to

$$\lambda(\gamma) \simeq \tan^{-1}[\tan\lambda_0 \cos^2\gamma],$$

where $\lambda_0 = \frac{1}{2}L_0/d_0$ is one half of the real seen radial period of the spiral along the fly-disk axis. For the approximation in the expression of $\gamma(\lambda)$, see Appendix 3.

There is therefore a set of angles

$$\gamma_n = \cos^{-1}\sqrt{\left(\frac{d_0}{L_0}\tan\frac{2\phi}{n}\right)} \quad (n = 1, \ldots)$$

and a corresponding set of circumferences on the spiral disk having radius

$$R_n = d_0 \tan\gamma_n = d_0 \tan\cos^{-1}\sqrt{\left(\frac{d_0}{L_0}\tan\frac{2\theta}{n}\right)} \quad (n = 1, \ldots)$$

on which reversal of motion occurs by Moiré effect. The spiral may be schematized as a set of concentric annular zones having width $R_n - R_{n-1}$, rotating alternately in the same and in the opposite sense with respect to the real rotation sense of the spiral, and therefore perceived as a pattern composed of alternate expanding and contracting zones. For this reason, for each set of spirals with the same radial period, i.e. radially equivalent,

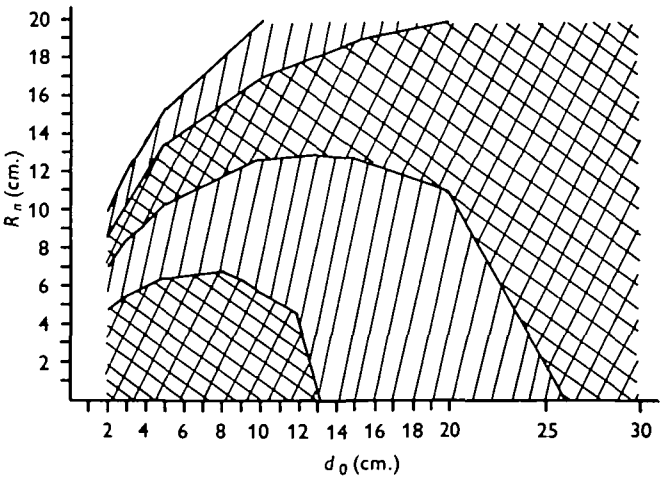

Fig. 9. Moiré reversal radii R_n and Moiré zones calculated, for spirals with $L = 1{\cdot}6$ cm. and for an interommatidic angle $\psi = 3{\cdot}5°$, by varying the fly-disk distance d_0.

it is possible to plot a diagram giving, for each distance from the eye of the fly to the spiral, the reversal points due to Moiré effect (Fig. 9).

A set of experiments has been performed to measure the influence of the Moiré effect on the landing reaction. The results were: (*a*) inside the ranges of distance and speed used, no fly ever reacted to an effective contraction, whatever were the pitch and

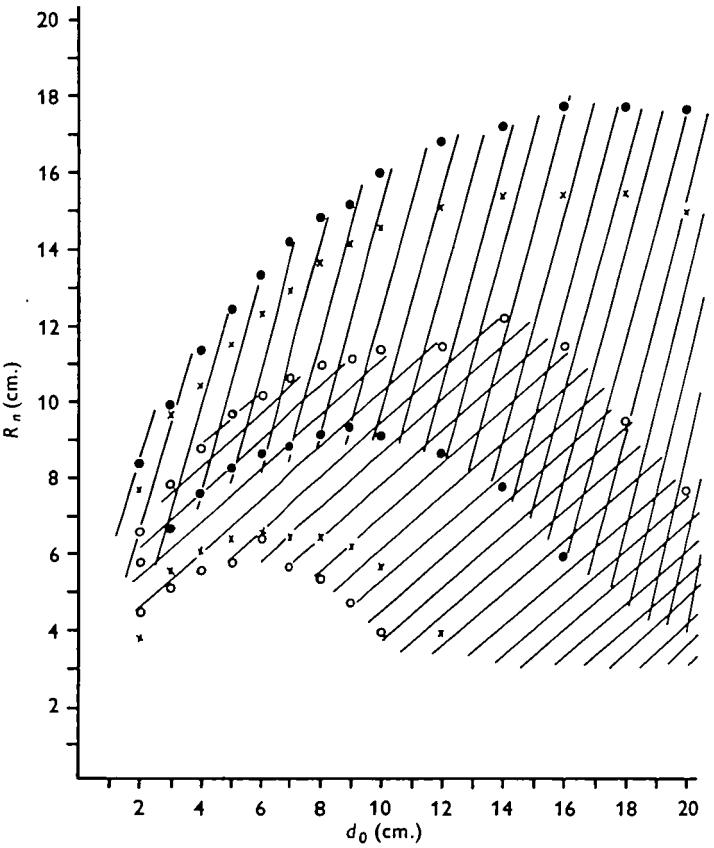

Fig. 10. Moiré reversal radii R_n and Moiré reduced zones (common to all interommatidic angles considered) calculated, for spirals with $L = 1{\cdot}6$ cm. and for interommatidic angles $\psi = 2{\cdot}5°$ (●), $3{\cdot}5°$ (×), $4°$ (○), by varying the fly-disk distance d_0.

the multiplicity of the spiral and the shape and the position of the stimulus, even if this stimulus was a ring completely included in a zone which, according to the above-mentioned diagrams, would have been theoretically a zone of expansion by Moiré effect; (*b*) no specific effect due to the adding of a Moiré zone was ever found; (*c*) the flies reacted to an effective expansion of rings completely included in a Moiré zone in which a contraction should have been perceived.

These results do not agree with the theoretical considerations developed above in the Moiré radial effect.

One may take into account the spread of values of interommatidic angles. The extreme values of these angles are (Vowles, 1966) $\phi = 2°$ and $\phi = 4{\cdot}6°$. In consequence of that spread of ϕ, there is a spread of Moiré zones (for each set of spirals with the same radial

period). Then one may consider the intersection of such zones in all such diagrams as reduced common Moiré zones (Fig. 10).

Not even in this case do the above-mentioned results agree with the theoretical considerations.

One has to note, as before, that the stimuli used have not only radial characteristics (for which the Moiré effect is valid, the effect depending on the intersection between radial periodicities of the eye and of the stimulus), and that by making use of the tangential characteristics the fly might avoid the confusion arising from the Moiré effect along the radius. This interpretation is in accordance with the existence of the above-mentioned tangential effects.

Third part

Several methods have been used in the study of the dependence of the landing reaction on the stimulated area and on the position of the stimulus in the visual field.

(*a*) The dependence of the reaction on the direction in which the pattern is presented to the fly has been studied.

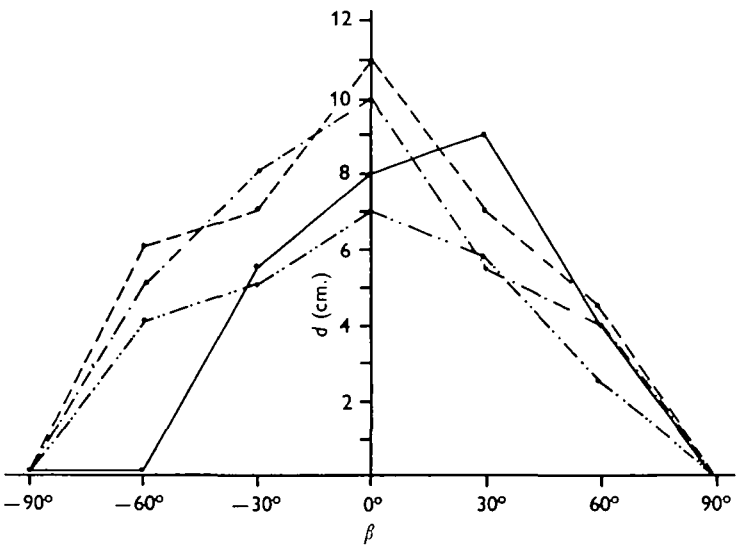

Fig. 11. Dependence of threshold value d of fly-disk distance on the angle β formed by the axis of the disk and the flight direction; radial expansion speed V_R = 55 cm./sec.; spiral 8/5.

For this purpose the whole disk has been moved around the fly, leaving the fly in front of the centre of the disk in the horizontal plane of flight. The direction of the stimulus is indicated by the angle β formed by the axis of the disk and the flight direction. The results are plotted in Fig. 11. The reaction is maximum for $\beta = 0°$, that is for an expansion arising in front of the fly, and there is no reaction for $\beta = 90°$. But if, always leaving $\beta = 90°$, the fly is displaced from the axis of the disk toward the periphery, facing the axis of the disk, then there is a zone of reaction.

(*b*) An interesting characteristic of the structure on which the landing reaction is based is the existence of preferential directions in the visual field.

In order to determine these directions, the rotating spiral has been presented to the fly through a horizontal slit having a length of 30 cm. and a width variable between

30 cm. and 2 mm. As shown in Fig. 12, as the width is reduced the stimulus efficiency decreases. The smallest slits for which reaction generally occurred were 3–4 mm. wide (but some flies reacted also with one 2 mm. wide). Slits 3–4 mm. wide have been presented at various angles (every 10°) with reference to a horizontal plane.

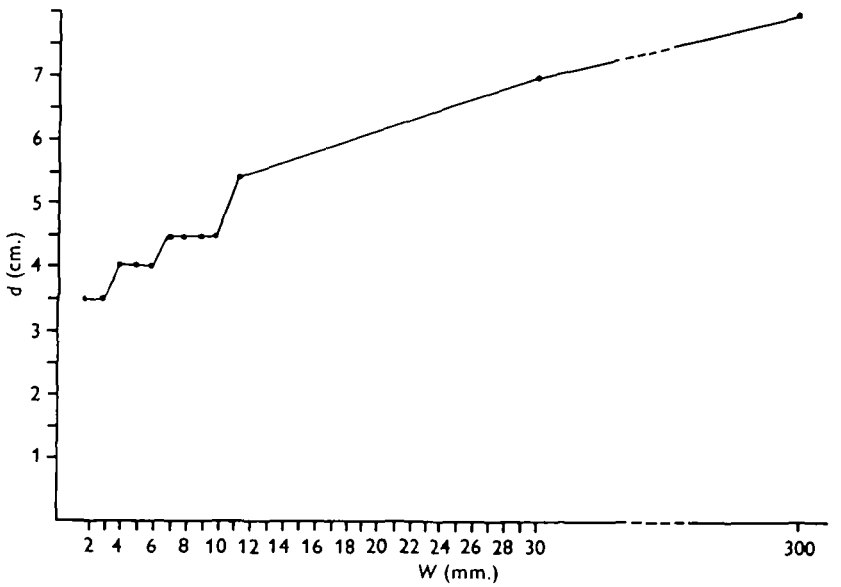

Fig. 12. Dependence of threshold value d of fly-disk distance on width w of an unidimensional stimulus (7–30 mm. and disk with a diameter of 30 cm.); radial expansion speed V_R = 16 cm./sec.; spiral 4·8/3.

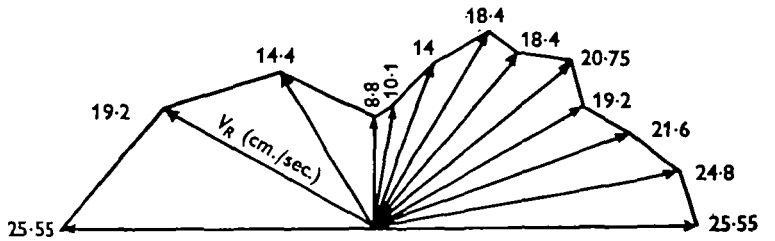

Fig. 13. Dependence of threshold value V_R of radial expansion speed on direction of a unidimensional stimulus (having width of 3 mm.) in the fly's visual field; fly-disk distance d = 9 cm.; spiral 8/1.

This experiment has been performed in two different ways: by fixing the rotation speed and reducing the distance in order to obtain the reaction, and by maintaining the fly at a fixed distance and increasing the rotation speeds until the fly reacts. Following both procedures, it was found that the vertical direction is the only preferred one. In fact any given slit is most efficient if it is vertical, other parameters being fixed (Fig. 13).

This higher efficiency of a vertical fissure having been noted, a set of experiments was performed to verify it.

A slit 30 cm. long and 1 cm. wide was shown, in the horizontal and in vertical positions, to the same flies situated at 10 cm. from the spiral (therefore the angle under

which the stimulus was seen was about 60), at three different speeds: 150, 180, 220 rev./min. (Table 1). From this table a clearly higher efficiency of the vertical slit may be deduced.

Table 1

Turning frequency (rev./min.)	Type of stimulus	Number of trials	Number of reactions	% of non-reaction
150	|	28	28	0
	—	28	19	32·14
180	|	28	18	35·71
	—	28	11	60·71
220	|	28	11	60·71
	—	28	5	82·14
Total	|	84	57	32·14
	—	84	35	58·33

Table 2

Number of stimuli of pre-adaptation	Type of stimulus	Number of trials	Number of non-reactions	% of non-reactions
0	|	21	1	4·76
	—	18	1	5·56
1	|	18	1	5·56
	—	18	10	55·6
2	|	15	8	55·33
	—	15	10	66·66
3	|	12	5	41·66
	—	12	10	83·33
4	|	9	6	66·66
	—	9	7	77·78
5	|	6	4	66·66
	—	6	6	100
6	|	3	2	66·66
	—	3	3	100

In order to avoid that the eventual reaction to a type of slit could depend on the training received, we calculated the percentages of the responses obtained after different types of stimuli had been shown. The results for each number of pre-adaptation stimuli are given in Table 2. From this it can be seen, in addition to the already observed higher efficiency of the vertical slit, that there is a reduction in the efficiency of both the vertical and horizontal stimuli with repetition.

(*c*) During the experiments performed at the beginning of this work in which only one side of the spiral was covered (Fig. 2), it has been found that the reaction is eliminated only if the pattern is covered up to 2·5 cm. beyond its centre (with the fly in front of the spiral centre as in all other experiments), independently of the direction of the rim of the covering mask. This leads one to think that, in this case, the stimulating pattern was perceived as a lateral displacement.

It was also thought that the moving pattern would be perceived as a lateral displacement rather than as an expansion, if the fly would see the rotating spiral through the

sector of a circle, of sufficiently small aperture. This has been experimentally obtained for sectors whose apertures are less than 155°, the value being the same whatever the direction of the rim of the covering mask. The value of 155° agrees well with the value of 161° obtainable from the experiment described in Fig. 2.

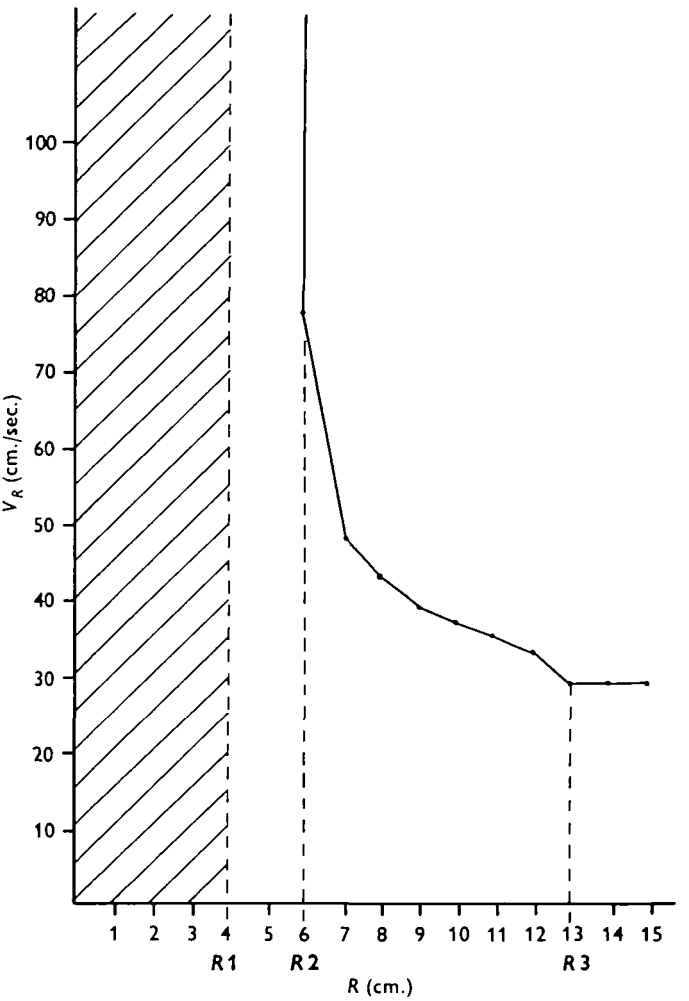

Fig. 14. Dependence of threshold value V_R of radial expansion speed on the external radius R of a stimulating annulus, for a fixed internal radius of the annulus $R1 = 4$ cm.; fly-disk distance $d = 15$ cm.; spiral 8/1; $R2$ = threshold excitatory external radius; $R3$ saturation external radius; $R2-R1$ = width of threshold excitatory stimulus; $R3-R1$ = width of saturation stimulus; $\overline{R1-R2}$ zone of deficient stimulation; $\overline{R2-R3}$ zone of proportionality; $\overline{R3-15}$ cm. zone of saturation.

(*d*) At the beginning of the work (Figs. 1, 2, 3) it was found on the disk that—after a central zone of proportionality between stimulus radius and stimulus efficiency—there was a maximum radius beyond which an increase of the stimulus radius was not followed by a corresponding increase of the stimulus efficiency.

To discover whether this maximum radius corresponds to the limits of the visual field of the fly as far as the landing reaction is concerned, the fly has been stimulated with rings of the disk all having internal radius greater than the maximum efficient radius. The results have shown that a stimulus lying external to the maximum efficient radius, if presented alone, is able to generate the landing reaction.

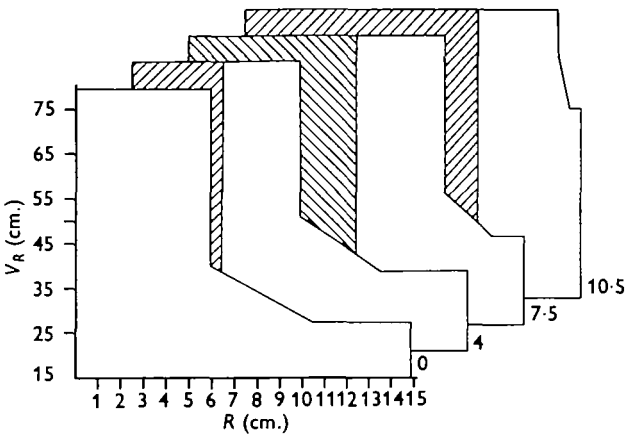

Fig. 15

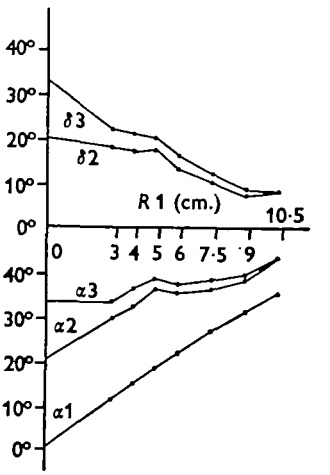

Fig. 16

Fig. 15. Dependence of experiments of the type described in Fig. 14 on internal radius $R1$ of stimulating annuli ($R1$ = 0, 4, 7·5, 10·5 cm.).

Fig. 16. The angle $\alpha 1$ at which the internal radius of a stimulating annulus is seen by the fly, the angle $\alpha 2$ at which the threshold excitatory external radius is seen, the angle $\alpha 3$ at which the saturation external radius is seen, the angle $\delta 2$ at which the threshold excitatory width is seen, and the angle $\delta 3$ at which the saturation width is seen, all as functions of the internal radius $R1$ of the stimulating annulus.

These two results, together, show a spatial integration of local landing stimuli that presents a phenomenon of saturation: the increase in size of the stimulus beyond a certain value does not generate an increase of the reaction.

It is to be recalled that another spatial summation effect was found in the experiments under (*b*) above (Fig. 12), in which the point of saturation was not reached because there were no experimental points for stimulus width between 3 and 30 cm.

The result of a typical experiment, using an annulus as stimulus is shown in Fig. 14. As the external radius of the stimulus (R) is increased, there is no reaction until a threshold point ($R2$) is reached; then there follows a zone in which the stimulus efficiency increases with the stimulus width, to reach a maximum (saturation point $-R3-$); thereafter the saturation zone follows.

The dependence of both threshold and saturation radii on the position of the stimulus in the visual field of the fly (indicated by the value of the internal radius of the stimulus $-R1-$) is obtained by varying both the internal and external radii of the opening in the mask between 0 and 15 cm. This is shown in Fig. 15. The variation of the parameters involved is reported in Fig. 16. As the internal radius is increased, both the angles $\alpha 2$ and $\alpha 3$ (under which the fly sees respectively the threshold and the saturation radii)

increase; and both the angles $\delta 2$ and $\delta 3$ (under which the fly sees respectively the threshold and the saturation widths) decrease. It is also to be noted that these two last curves converge, showing that the proportionality zone, given by their difference, decreases.

One may note that the value of the angle, under which the fly sees the stimulus at the shortest distance in Fig. 3 (that is $\tan^{-1} \frac{1}{2}\phi/d = 26°$), agrees well with the corresponding average value of 20° obtained for $R\,1 = 0$ in Fig. 16.

Successive analysis of this spatial integration of local stimuli, together with the results on the temporal organization of stimuli reported in the first part and in Appendix 2, and their comparison with anatomical data on the visual system of flies (Cajal & Sanchez, 1915; Braitenberg, 1967; Trujillo-Cenóz & Melamed, 1966; Kirschfeld, 1967) will lead to a model of the functional structure underlying the landing reaction and its relation with models of movement perception.

SUMMARY

1. The house-fly exhibits the landing reaction when an expanding optical pattern is placed before it.

An expanding pattern which is easy to measure and which keeps the level of illumination constant is created by rotating spirals.

2. In analysing the dependence of landing reaction on the spiral pitch and multiplicity and on the frequency of local stimuli on each ommatidium, (*a*) interference by the tangential characteristics of the spiral has been observed; (*b*) stimulus efficiency has been found to depend on stimulus wave-length; (*c*) the relevance of the above factors and of a temporal parameter influencing both optomotor and landing reactions has been evaluated.

3. The fact that no Moiré effect has been observed is explained in terms of characteristics of stimuli used.

4. The dependence of pattern efficiency on the position of the stimulus in the visual field has been ascertained.

5. Spatial integration of local landing stimuli has been shown in various cases and its threshold excitability and saturation point have been obtained. The dependence of these two last parameters on the position of the stimulus in the visual field has been ascertained.

APPENDIX 1

The parametric equation of the arithmetic spiral of pitch p is

$$x(\theta) = r\cos\theta = \frac{p}{2\pi}\theta\cos\theta,$$

$$y(\theta) = r\sin\theta = \frac{p}{2\pi}\theta\sin\theta.$$

The equation of its tangent in the point (x_0, y_0) is

$$y - y_0 = \frac{[dy/d\theta]_{y_0}}{[dx/d\theta]_{x_0}}(x - x_0).$$

The slope of the normal to the spiral will be

$$m_{n_s} = \frac{-1}{m_\tau}, \quad \text{where} \quad m_\tau = \frac{[dy/d\theta]_{x_0}}{[dx/d\theta]_{y_0}}$$

is the slope of the tangent. So, ξ_{n_s} being the angle that the normal to the spiral forms with the x axis,

$$\tan \xi_{n_s} = m_{n_s} = -\frac{[dx/d\theta]_{y_0}}{[dy/d\theta]_{x_0}},$$

where

$$\frac{dx}{d\theta} = \frac{d}{d\theta}\left(\frac{p}{2\pi}\theta\cos\theta\right) = \frac{p}{2\pi}(\cos\theta - \theta\sin\theta),$$

$$\frac{dy}{d\theta} = \frac{d}{d\theta}\left(\frac{p}{2\pi}\theta\sin\theta\right) = \frac{p}{2\pi}(\sin\theta + \theta\cos\theta),$$

then

$$\tan \xi_{n_s} = \frac{\theta\sin\theta - \cos\theta}{\theta\cos\theta + \sin\theta}.$$

The normal to a circumference is its radius, so its slope is

$$m_{n_c} = \tan \zeta_{n_c} = \tan\theta,$$

where ζ_{n_c} is the angle that such a normal forms with the x axis.

Now the angle between the two curves, that is the angle between the two normals, is

$$\tan\mu = \tan(\xi_{n_c} - \zeta_{n_s}) = \frac{\tan\zeta_{n_c} - \tan\zeta_{n_s}}{1 + \tan\zeta_{n_c}\tan\xi_{n_s}} = \frac{\dfrac{\sin\theta}{\cos\theta} - \dfrac{\theta\sin\theta - \cos\theta}{\theta\cos\theta + \sin\theta}}{1 + \dfrac{\sin\theta}{\cos\theta}\dfrac{\theta\sin\theta - \cos\theta}{\theta\cos\theta + \sin\theta}} = \frac{1}{\theta} = \frac{p}{2\pi r},$$

i.e.

$$\mu = \tan^{-1}\frac{p}{2\pi r}.$$

This angle increases with pitch and decreases with increase of radius.

The variation of μ with r is given by

$$\frac{\partial\mu}{\partial r} = \frac{\partial\mu}{\partial\tan\mu}\frac{\partial\tan\mu}{\partial r} = \frac{1}{\dfrac{\partial\tan\mu}{\partial\mu}}\frac{\partial r}{\partial\tan\mu},$$

where

$$\frac{\partial\tan\mu}{\partial\mu} = \frac{1}{\cos^2\mu} \quad \text{and} \quad \frac{\partial\tan\mu}{\partial r} = \frac{\partial}{\partial r}\left(\frac{p}{2\pi r}\right) = \frac{-p}{2\pi r^2},$$

then

$$\frac{\partial\mu}{\partial r} = \frac{-p}{2\pi r^2}\cos^2\mu = \frac{-p}{2\pi r^2}\left(\frac{1}{\sqrt{(1+\tan^2\mu)}}\right)^2 = \frac{-p/2\pi}{r^2 - (p/2\pi)^2} = \frac{-r/\theta}{r^2 - (r/\theta)^2}$$

$$= \frac{-\theta/r}{\theta^2 - 1} = \frac{-2\pi/p}{(2\pi r/p)^2 - 1} = \frac{-2\pi p}{(2\pi r)^2 - p^2}.$$

This function evidently decreases with increasing radius; moreover it increases with increasing p, its derivative with respect to p being everywhere positive:

$$\frac{\partial}{\partial p}\left(\frac{\partial\mu}{\partial r}\right) = \frac{[(2\pi r)^2 - p^2]\,2\pi - (2\pi p)(-2p)}{[(2\pi r)^2 - p^2]^2} = \frac{2\pi[(2\pi r)^2 + p^2]}{[(2\pi r)^2 - p^2]^2}.$$

APPENDIX 2

The experiments of the first part show that stimulus efficiency decreases both by increasing m or p, as is schematized in Fig. 17. Recall that: (*a*) the same V_R is obtainable with spirals of different p; (*b*) the same number of stimuli per unit time on the same

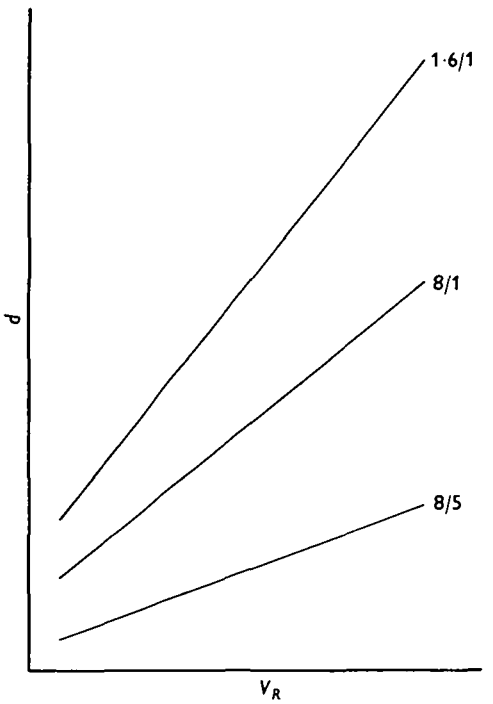

Fig. 17. Schematic diagram of experiments on the dependence of threshold value d of fly-disk distance on radial expansion speed V_R, for two different values of pitch (p = 1·6, 8 cm.) and of multiplicity (m = 1, 5).

ommatidium may be obtained at the same V_R by spirals differing by p, but not by L; (*c*) in using spirals as expanding patterns the existence of two sources of interference (tangential and torsion effects) is implicit. The amount of such interference is constant if p is not changed.

Let T_1 be the time necessary for a stimulus to pass from one ommatidium to the adjacent ommatidium. This time is the sole cause of any movement detection in Reichardt's model describing stimulus-reaction relations of optomotor responses (Reichardt, 1962).

Let T_2 be the time necessary for two successive stimuli to reach an ommatidium: $T_2 = [(p/m)/2]/V_R$. The variation of this time is the cause of the spread of curves showing the direct proportionality of optomotor reaction and stimulus wavelength in other experiments (Graffon, 1934; Fig. 6 of Fermi & Reichardt, 1963 and Fig. 7*a* of Bishop & Keehn, 1967).

Note that:

(I) The efficiency of stimulating patterns increases with the increase of T_2 and with the decrease of T_1 and of interference.

(II) If, on the curve of any single spiral (Fig. 17), one passes from one point to another, as V_R increases both T_1 and T_2 decrease and interference remains constant.

(III) If one passes from the curve corresponding to one spiral to another with the same p, leaving V_R = const. (Fig. 17), as m decreases (i.e. from 8/5 to 8/1) T_1 remains constant, T_2 increases and interference remains constant.

(IV) If one passes from the curve corresponding to one spiral to another with the same m, leaving V_R = const. (Fig. 17), as p decreases (i.e. from 8/1 to 1·6/1) T_1 remains constant, T_2 decreases and the interference also decreases.

(V) If one passes from the curve corresponding to one spiral to another with the same L, leaving V_R = const. (Fig. 17), as both p and m decrease (i.e. from 8/5 to 1·6/1) both T_1 and T_2 remain constant and the interference decreases.

(VI) If one passes from a point at speed V_{Ri} on the curve corresponding to a spiral p_i, m_i, to a point at speed V_{Rj} on the curve corresponding to a spiral p_j, m_j (Fig. 17), T_2 varies as

$$T_{2j} = \gamma T_{2i},$$

where

$$\gamma = \frac{T_{2j}}{T_{2i}} = \frac{p_j/m_j}{V_{Rj}} \Big/ \frac{p_i/m_i}{V_{Ri}}.$$

The motion-detecting cells in optic ganglia are systems in which several inputs are weighted differently in effectiveness (Bullock & Horridge, 1965).

The relevance the fly ascribes, for landing reaction, to the three above-mentioned parameters (T_1, T_2, interference) will be obtained from the fly's responses at different p, m and V_R.

To compare the relevance for the fly of the variations of two of the three parameters, it is necessary to leave the third one constant.

(1) T_1 *and* T_2. Interference remains constant if the spiral is not changed (see *c*). Take two points at different V_R on a single spiral curve (Fig. 17). As V_R increases T_1 and T_2 decrease (see II). These decrements are in percentage the same. As stated in I, a decrease of T_1 raises pattern efficiency and a decrease of T_2 depresses it. Experiments (Fig. 17) show that as V_R increases pattern efficiency increases. Then T_1 variation is more relevant than T_2 variation.

(2) T_2 *and interference*. T_1 remains constant if V_R is constant. Take two curves of spirals with the same m, differing in p, and, on each of them, a point at the same V_R (Fig. 17). As p decreases T_2 and interference decreases (see IV). As stated in I, a decrease of T_2 depresses pattern efficiency and a decrease of interference raises it. Experiments (Fig. 17) show that as p decreases pattern efficiency increases. Then interference variations are more relevant than T_2 variation.

(3) T_1 *and interference*. T_2 remains constant if $\gamma = 1$. Take two curves of spirals with the same m, and, on each of them, a point at different V_R, such that when V_R decreases p also decreases (Fig. 17). As V_R decreases T_1 and T_2 increase (see II). As p decreases T_2 and interference decrease (see IV). T_2 remains constant when

$$1 = \gamma = V_{Ri} \cdot p_j / V_{Rj} \cdot p_i$$

(see VI), that is, when the radial speeds of the two points are directly proportional to the pitches of spirals to which they belong. As stated in I, an increase of T_1 depresses

pattern efficiency and a decrease of interference raises it. Experimental data in such conditions ($\gamma = 1$) show that as V_R and p decrease pattern efficiency decreases. Then T_1 variation is more relevant than interference variations.

We have to add in finishing that in Fig. 6 of Fermi & Reichardt (1963), (1) along each curve varying V_R, T_1 and T_2 change simultaneously and by the same amount; (2) along a line of constant V_R, passing from one curve to another, T_1 remains constant and T_2 varies in the same sense as the stimulus wavelength; in both cases there is no interference; in the present experiments in (iii) for each V_R, T_1 remains constant, T_2 varies in the same sense as the stimulus wavelength and the existing interference does not change. So the only difference from (2) is the existence of a certain constant amount of interference; this constant interference changes the zero position of the efficiency axis, but not the relative position of curves in diagrams; in (ii) for each V_R, there is a change of interference and so the relative position of the curves is varied.

Comparing the results herein reported with the results obtained by other workers, the disagreement under (ii) and the agreement under (iii) are explained by the considerations outlined above.

APPENDIX 3

The relative error incurred by assuming the spatial angle covered by the projection of the seen surface on the normal plane, i.e. $2\lambda(\gamma)$, in place of the real spatial angle covered by the seen surface, i.e. $\lambda_1+\lambda_2$ (in Fig. 8 taking AC in place of BD), is

$$\epsilon = \frac{BD-AC}{BD} = \left(1-\frac{AC}{BD}\right) = 1-\rho,$$

$$\text{with } \rho = AC/BD.$$

This error, in every case in our experiments, is only a few percent, reaching 10% in some rare cases.

In fact:

L 1. In Fig. 8:

$$PE = PF = \tfrac{1}{2}L, \qquad QF = d_0 \tan(\gamma-\lambda_1),$$
$$QP = d_0 \tan\gamma, \qquad QE = QP+PE,$$
$$QE = d_0 \tan(\gamma+\lambda_2), \qquad QF = QP-PF,$$

substituting

$$d_0 \tan(\gamma+\lambda_2) = d_0 \tan\gamma + \tfrac{1}{2}L, \quad d_0 \tan(\gamma-\lambda_1) = d_0 \tan\gamma - \tfrac{1}{2}L.$$

If λ_0 is the angle under which $\frac{1}{2}L$ is seen at distance d_0 in the centre of the disk, it will be $\tan\lambda_0 = L/2d_0$. Then

$$\tan\gamma + \tan\lambda_0 = \tan(\gamma+\lambda_2) = \frac{\tan\gamma+\tan\lambda_2}{1-\tan\gamma\tan\lambda_2},$$

$$\tan\gamma - \tan\lambda_0 = \tan(\gamma-\lambda_1) = \frac{\tan\gamma-\tan\lambda_1}{1+\tan\gamma\tan\lambda_1}.$$

That is

$$\tan\lambda_1 = \frac{\tan\lambda_0}{1+\tan^2\gamma-\tan\gamma\tan\lambda_0}, \quad \tan\lambda_2 = \frac{\tan\lambda_0}{1+\tan^2\gamma+\tan\gamma\tan\lambda_0}$$

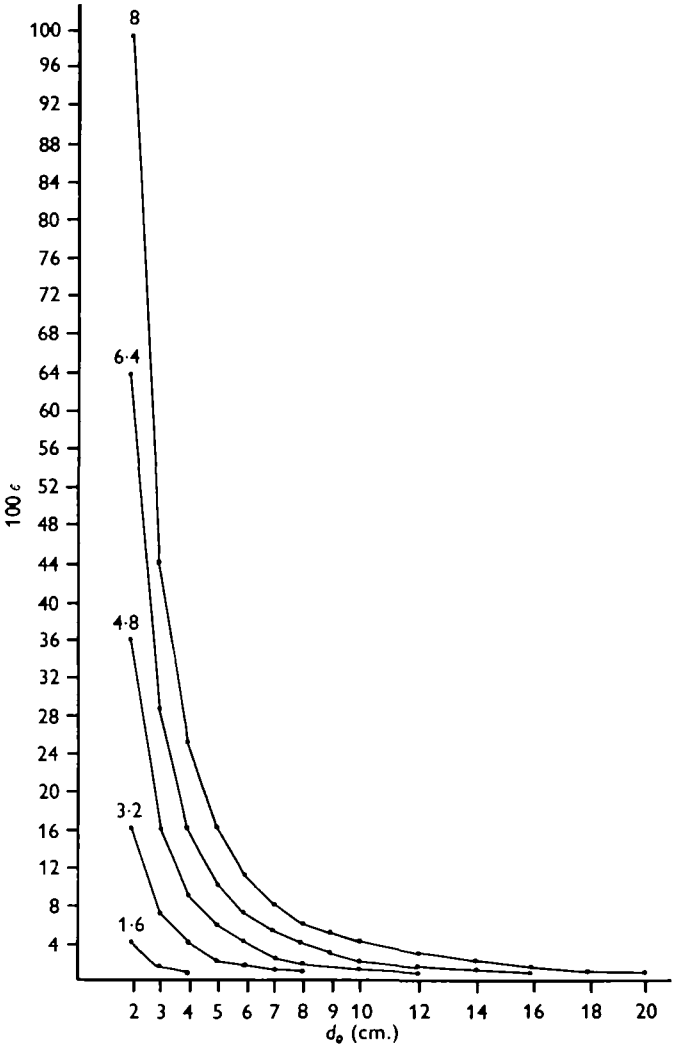

Fig. 18. Percentage error 100ϵ, incurred by assuming in Fig. 8 $2\lambda(\gamma)$ in place of $\lambda_1+\lambda_2$, calculated for various spiral radial periods (L = 1·6, 3·2, 4·8, 6·4, 8·0 cm.) by varying the fly-disk distance d_0. $100\epsilon = 25(L/2d_0)^2$.

L (cm.)					
1·6	3·2	4·8	6·4	8	d_0 (cm.)
4	16	36	64	100	2
1·78	7·12	16	28·48	44·2	3
1	4	9	16	25	4
	2·56	5·76	10·24	16	5
	1·77	4	7·1	11·1	6
	1·3	2·94	5·22	8·16	7
	1	2·25	4	6·25	8
		1·8	3·2	5	9
		1·44	2·56	4	10
		1	1·77	2·8	12
			1·52	2·04	14
			1	1·55	16
				1·25	18
				1	20

and
$$\tan\lambda_1+\tan\lambda_2=\frac{\tan\lambda_0}{(1+\tan^2\gamma)-\tan\gamma\tan\lambda_0}+\frac{\tan\lambda_0}{(1+\tan^2\gamma)+\tan\gamma\tan\lambda_0}$$
$$=\frac{2\tan\lambda_0}{(1+\tan^2\gamma)-\dfrac{\tan^2\gamma\tan^2\lambda_0}{1+\tan^2\gamma}}$$
$$=\frac{2\tan\lambda_0}{\dfrac{1}{\cos^2\gamma}-\sin^2\gamma\tan^2\lambda_0}$$
$$=\frac{2\tan\lambda_0\cos^2\gamma}{1-\sin^2\gamma\cos^2\gamma\tan^2\lambda_0}$$
$$=\frac{2\tan\lambda_0\cos^2\gamma}{1-\frac{1}{4}\sin^2 2\gamma\tan^2\lambda_0}.$$

L 2. In Fig. 8:

$$AP=EP\cos\gamma=\tfrac{1}{2}L\cos\gamma,\quad PC=FP\cos\gamma=\tfrac{1}{2}L\cos\gamma,$$
$$OP=OQ/\cos\gamma=d_0/\cos\gamma,$$
$$\frac{AC}{OP}=\frac{AP+PC}{OP}=\frac{\frac{1}{2}L\cos\gamma+\frac{1}{2}L\cos\gamma}{d_0/\cos\gamma}=2\tan\lambda_0\cos^2\gamma.$$

L 3.
$$\rho=\frac{AC}{BD}=\frac{AC/OP}{BD/OP}=\frac{2\tan\lambda_0\cos^2\gamma}{\tan\lambda_1+\tan\lambda_2}=\frac{2\tan\lambda_0\cos^2\gamma}{\dfrac{2\tan\lambda_0\cos^2\gamma}{1-\frac{1}{4}\sin^2 2\gamma\tan^2\lambda_0}}=1-\tfrac{1}{4}\sin^2 2\gamma\tan^2\lambda_0,$$

substituting
$$\epsilon=1-\rho=1-(1-\tfrac{1}{4}\sin^2 2\gamma\tan^2\lambda_0)=\tfrac{1}{4}\sin^2 2\gamma\tan^2\lambda_0.$$

L 4.

The maximum relative error will be for $\sin 2\gamma=1$ ($\gamma=45°$)
$$\epsilon_{\max.}=\tfrac{1}{4}\tan^2\lambda_0=\tfrac{1}{4}(L/2d_0)^2.$$

In Fig. 18 are reported the Table and the diagram of the percentage error 100ϵ for the various spiral radial periods at several distances.

Now, the maximum radial period used has been $L=8$ cm. and the minimum distance attained with such a spiral has been of the order of 6–8 cm. For these data Fig. 18 gives a percentage error $\epsilon\simeq 11\,\%\div 6\,\%$, q.e.d.

ACKNOWLEDGEMENTS

We thank Professor Valentino Braitenberg (present address: Max Plank Institut für biologische Kybernetik, Tübingen) for having suggested the present research and supported it with fruitful criticisms and discussions, Dr Uja Pinardi Vota for her valuable collaboration in performing part of the experiments and the Laboratorio di Parassitologia of the Istituto Superiore di Sanità of Roma for supplies of flies. This research was sponsored in part by EOAR 68-0030.

REFERENCES

BISHOP, L. G. & KEEHN, D. G. (1967). Neural correlates of the optomotor response in the fly. *Kybernetik* **3**, 288–95.

BRAITENBERG, V. (1967). Patterns of projection in the visual system of the fly. I. Retina–lamina projection. *Exp. Brain Res.* **3**, 271–98.

BRAITENBERG, V. & TADDEI FERRETTI, C. (1966). Landing reaction of *Musca domestica*. *Naturw.* **53**, (6), 155–6.

BULLOCK, T. H. & HORRIDGE, G. A. (1965). Structure and Function in the Nervous System of Invertebrates. San Francisco: W. H. Freeman.

BURTT, E. T. & CATTON, W. T. (1954). Visual perception of movement in the locust. *J. Physiol.* **125**, 566–80.

CAJAL, S. R. & SANCHEZ, D. (1915). Contribuciòn al conocimiento de los centros nerviosos de los insectos. *Trab. Lab. Invest. biol. Univ. Madr.* **13**, 1–16.

FERMI, G. & REICHARDT, W. (1963). Optomotorische Reaktionen der Fliege *Musca domestica*. *Kybernetik* **2**, 15–28.

GOODMAN, L. J. (1960). The landing responses of insects. I. The landing response of the fly, *Lucilia sericata* and other Calliphorinae. *J. exp. Biol.* **37**, 854–78.

GOODMAN, L. J. (1964). The landing responses of insects. II. The electrical responses of the compound eye of the fly *Lucilia sericata*, upon stimulation by moving objects and slow changes of light intensity. *J. exp. Biol.* **41**, 403–13.

GÖTZ, C. G. (1964). Optomotorische Untersuchung der visuallen System einiger Augenmutanten der *Drosophila*. *Kybernetik* **2**, 77–92.

GRAFFON, M. (1934). Untersuchungen über das Bewegungssehen bei Libellenlarven, Fliegen und Fischen. *Z. vergl. Physiol.* **20**, 299–337.

HASSENSTEIN, B. & REICHARDT, W. (1956). Systemtheoretische Analyse der Zeit-, Reihenfolgen- und Vorzeichenauswertung bei der Bewegungsperzeption des Rüsselkäfers Clorophanus. *Z. Naturf.* **11** b, 513–24.

HERTZ, M. (1934*a*). Zur Physiologie des Formen- und Bewegungssehen. I. Optomotorische Versuche an Fliegen. *Z. vergl. Physiol.* **20**, 430–49.

HERTZ, M. (1934*b*). Zur Physiologie des Formen—und Bewegungssehen. II. Auflösungs vermögen des Bienenauges und optomotorische Reaktion. III. Figurale Unterscheidung und reriproke Dressuren bei der Biene. *Z. vergl. Physiol.* **21**, 579–615.

HORRIDGE, G. A. (1966). Study of a system as illustrated by the optokinetik response. *Symp. Soc. exp. Biol.* **20**, 179–98.

HORRIDGE, G. A. (1968). Interneurons. San Francisco: W. H. Freeman.

KIRSCHFELD, K. (1967). Die Beziehung zwischen dem Raster der Ommatidien und dem Raster der Rhabdomere im Komplexauge von Musca. *Exp. Brain Res.* **3**, 248–70.

MCCANN, G. B. & MCGINITIE, G. F. (1965). Optomotor response studies of insect vision. *Proc. Roy. Soc. Lond.* B **163**, 369–401.

RAYLEIGH, J. W. S. LORD (1874). On the manufacture and theory of diffraction gratings. *London, Edinburgh and Dublin Philosophical Magazine and Journal of Science*, series 4, **47**, 310, 8193.

REICHARDT, W. (1962). Nervous integration in the facet eye. *Biophys. J.* **2**, 121–43.

REICHARDT, W. & VARJÚ, D. (1959). Übertragungseigenschaften in Auswertensystem für das Bewegungssehen. *Z. Naturf.* **14**, 674–89.

TADDEI FERRETTI, C. & FERNANDEZ PEREZ DE TALENS, A. (1967). La reazione d'atterraggio della *Musca domestica*. *Atti Congr. Naz. Cibernetica Pisa* pp. 37–42.

THORSON, J. (1966). Small-signal analysis of a visual reflex in the locust. I. Input parameters; II. Frequency dependence. *Kybernetik* **3**, 41–66.

TRUJILLO-CENÓZ, O. & MELAMED, J. (1966). Compound eye of dipterans: Anatomical basis for integration. An electron microscope study. *J. Ultrastruct. Res.* **16**, 395–98.

VOWLES, D. M. (1966). The receptive fields of cells in the retina of the house-fly (*Musca domestica*). *Proc. Roy. Soc. Lond.* B **164**, 552–70.

WALLACE, G. K. (1959). Visual scanning in the desert locust Schistocerca Gregaria Forskäl. *J. exp. Biol.* **36** (3), 512–25.

LIST OF SYMBOLS USED IN FIGURES

d, threshold value of fly's distance from the disk; D, distance, from the centre of the disk, of a vertical chord limiting a circular segment; V_R, threshold value of radial speed of expansion; spiral x/y, spiral having pitch of x cm. and multiplicity y; ϕ, diameter of stimulating pattern; p, pitch of the spiral; m, multiplicity; L, radial period of the spiral ($L = p/m$); w, width of a unidimensional stimulus; γ, angle between the axis of an ommatidium and the fly-disk axis; $\lambda_1 + \lambda_2$, radial period of the spiral seen by an ommatidium whose axis is at angle γ with the fly-disk axis; $d_0 = d(0)$, fly-disk distance; $d(\gamma)$, fly-disk distance along the axis of an ommatidium, the axis being at angle γ with the fly-disk axis; $L_0 = L(0)$, radial period of the spiral $= L$; $L(\gamma)$, projection of the radial period of the spiral on the plane of an ommatidium whose axis is at angle γ with the fly-disk axis; λ_0, half of the radial period of the spiral seen along the fly-disk axis; $\lambda(\gamma)$, projection of half of the radial period of the spiral on the plane of an ommatidium, whose axis is at angle γ with the fly-disk axis, as seen by that ommatidium; R_n, n^{th}, Moiré reversal radius at distance d_0; ψ, interommatidic angle; β, angle formed by the axis of the disk and the flight direction; 1006, percentage error; R, external radius of a stimulating annulus; $R1$, internal radius of a stimulating annulus; $R2$, threshold excitatory external radius of a stimulating annulus; $R3$, saturation external redius of a stimulating annulus; $\alpha 1$, angle at which the fly sees the internal radius of a stimulating annulus; $\alpha 2$, angle at which the fly sees the threshold excitatory external radius of a stimulating annulus; $\alpha 3$, angle at which the fly sees the saturation external radius of a stimulating annulus; $\delta 2$, angle at which the fly sees the threshold excitatory width of a stimulating annulus; $\delta 3$, angle at which the fly sees the saturation width of a stimulating annulus.